Chinese Journal of
POLYMER SCIENCE

RESEARCH ARTICLE

https://doi.org/10.1007/s10118-026-3698-2
Chinese J. Polym. Sci.

Epoxy-functionalized Cyclohexane-based Ricinoleate Plasticizer: Synthesis, Performance Evaluation, and Plasticizing Mechanism

Zhuo-Kai Wang[a,b], Ying-Yong Jiang[c], Wen-Nan Du[a,b], Yao-Bin Wang[a,b], Xing-Chen Bai[a,b], Cheng-Wei Song[a,b], Zhi-Peng Jiang[a,b], Liang Ren[a,b*], Sai-Nan Cui[a,b], and Feng-Xiang Gao[d*]

[a] *School of Chemical Engineering, Changchun University of Technology, Changchun 130102, China*
[b] *Engineering Research Center for synthetic resin and special fiber, Ministry of Education, Changchun University of Technology, Changchun 130102, China*
[c] *Research Institute of Jilin Petrochemical Company, PetroChina, Jilin 132012, China*
[d] *Key Laboratory of Polymer Ecomaterials, Changchun, Institute of Applied Chemistry CAS, Chinese Academy of Sciences, Changchun 130022, China*

Abstract The molecular design of bio-based plasticizers often involves a trade-off between key performance and sustainability. Herein, we propose a novel molecular design strategy that breaks this contradiction by integrating a flexible backbone derived from non-edible sources, sustainable alicyclic rigid core, and epoxy groups. A series of epoxy-functionalized cyclohexane-based ricinoleate plasticizers, epoxyacetyl ricinoleic acid cyclohexanol ester (EACHR), epoxyacetyl ricinoleic acid cyclohexanediol ester (EACHDR), and epoxyacetyl ricinoleic acid cyclohexanedimethanol ester (EACHDMR), were synthesized. When evaluated in poly(vinyl chloride) (PVC) as a demanding validation platform, the optimal plasticizer (EACHDMR) achieved comprehensive performance, which reduced the glass transition temperature (T_g) by 30%, increased the elongation at break by more than 50-fold, and enhanced the notched impact strength by over 35-fold compared to an unplasticized PVC sample. Importantly, EACHDMR exhibited lower migration and 20.7% higher plasticizing efficiency than the commercial benchmark dioctyl terephthalate (DOTP). This study demonstrated that by rationally integrating rigid cores, flexible fatty acid chains, and polar groups, it is possible to successfully balance performance and sustainability, providing a new design strategy for developing high-performance and sustainable alternatives to traditional plasticizers.

Keywords Bio-based plasticizer; Epoxy-functionalization; Molecular design; Plasticizing efficiency; Sustainability

Citation: Wang, Z. K.; Jiang, Y. Y.; Du, W. N.; Wang, Y. B.; Bai, X. C.; Song, C. W.; Jiang, Z. P.; Ren, L.; Cui, S. N.; Gao, F. X. Epoxy-functionalized cyclohexane-based ricinoleate plasticizer: synthesis, performance evaluation, and plasticizing mechanism. *Chinese J. Polym. Sci.* https://doi.org/10.1007/s10118-026-3698-2

INTRODUCTION

Plasticizers are important for endowing flexible polymer materials. Therefore, it is widely used in the preparation of various commercial products. Among these plasticizers, traditional petroleum-based phthalates have dominated the market owing to their low cost and effective performance.[1,2] However, this dominance remains a significant challenge. Substantial evidence indicates that these compounds migrate readily from products, posing established risks to human health and the environment.[3–5] This has led to increasingly strict global regulations.[6] Consequently, these regulatory pressures, along with the constraint of the unsustainability of fossil resources, have driven an urgent need for novel, non-toxic plasticizers derived from renewable biomass.[7–9]

To address this need, bio-based alternatives have become the primary candidates derived from abundant and renewable resources. However, the inherent limitations of molecular design have hindered their widespread commercial application.[10–12] Specifically, current designs typically struggle to achieve key performances simultaneously, such as plasticizing efficiency and migration resistance. This may not achieve a good overall performance. For instance, linear polyol esters from soybean oil achieve higher thermal stability at the expense of mechanical strength.[13,14] However, rigid cyclic structures based on petrochemical benzene rings enhance compatibility while compromising both sustainability and safety owing to toxicity risks.[15–17] Beyond these molecular design issues, dependence on food-competing feedstocks, such as edible oils, raises ethical concerns and supply chain risks.[18,19] Consequently, bio-based plasticizers currently account for less than 10% of the market and are yet to meet comprehensive commercial performance standards.[20,21]

To overcome these challenges, we propose a molecular design strategy that combines three key elements to enhance polymer interactions: a flexible backbone derived from non-edible sources, a sustainable alicyclic rigid core, and polar functional groups. For the flexible backbone, ricinoleic acid (RA), a natural hydroxy fatty acid from castor oil, was selected because of its proven low toxicity and chemical

* Corresponding authors, E-mail: renl@ccut.edu.cn (L.R.)
E-mail: gfx26@ciac.ac.cn (F.X.G.)
Received January 28, 2026; Accepted April 4, 2026; Published online October 10, 2026

functionality.[22–25] For the rigid core, a bio-derivable cyclohexane ring was introduced to replace the benzene ring. This structure offers significant steric hindrance and polarity similar to aromatic rings but does not possess the corresponding toxicity, conforming to the principles of green chemistry.[26,27] In addition, the molecule is functionalized with epoxy groups to strengthen the dipole-dipole interactions with polar polymer chains.[28] Therefore, we hypothesize that this synergistic "RA-cyclohexane-epoxy" design will achieve a balance in plasticizing efficiency, migration resistance, and thermomechanical performance.

To test this hypothesis, we synthesized a series of epoxy-functionalized cyclohexane-based ricinoleate plasticizers (EACHR, EACHDR, and EACHDMR). Subsequently, poly(vinyl chloride) (PVC) was selected as a strict validation platform because of its high polarity and strong intermolecular forces, which make it an exceptionally demanding matrix for assessing plasticizer performance.[29–31] On this platform, the thermal stability, mechanical properties, migration resistance, and plasticizing efficiency of PVC plasticized with the compounds were systematically evaluated and benchmarked against dioctyl terephthalate (DOTP). Thus, this work not only presents high-performance alternatives but also provides insights into the molecular design of sustainable plasticizers.

MATERIALS AND METHODS

Materials

Poly(vinyl chloride) (PVC, grade SG-5) was sourced from Xinjiang Tianye Co., Ltd. (China). Ricinoleic acid (AR, ≥99.0%), 1,4-cyclohexanediol (AR, ≥99.5%), cyclohexanol (AR, ≥99.5%), 1,4-cyclohexanedimethanol (AR, ≥99.5%), and *p*-toluenesulfonic acid (AR, ≥99.0%) were purchased from Shanghai Macklin Biochemical Co., Ltd. (China). Sodium bicarbonate (AR, ≥99.5%), toluene (AR, ≥99.5%), and formic acid (≥88 wt%), hydrogen peroxide (30 wt%), and ethyl acetate (AR, ≥99.0%) were supplied by Tianjin Guangfu Technology Development Co., Ltd. (China). Dioctyl terephthalate DOTP (industrial grade, ≥99.0%) and methyltin mercaptide stabilizer (CP, ≥98%) were obtained from Shandong Blue Sail Chemical Co., Ltd. (China).

Synthesis of Epoxyacetyl Ricinoleic Acid Cyclohexanol Ester (EACHR)

Ricinoleic acid (298.46 g, 1 mol), and acetic anhydride (122.51 g, 1.2 mol) were charged into a three-necked flask under a nitrogen atmosphere. The mixture was then stirred and heated at 140 °C for 2 h. After cooling to room temperature, the crude product was washed with deionized water until the aqueous washings were neutral. It was then purified by distillation under reduced pressure to obtain the refined acetylated ricinolate (AR) product.

AR (340 g, 1 mol), p-toluenesulfonic acid (5.7 g, 0.03 mol), cyclohexanol (110.17 g, 1.1 mol), and the appropriate amount of toluene as an aqueous agent were added to a three-necked round-bottomed flask with a condensate refluxing device and a stirring device. After the component reagents were fully dissolved, the reaction was performed at 120 °C under a nitrogen atmosphere. The reaction continues for 10–12 h until the water yield approached the theoretical value. At the end of the reaction, the product was cooled to room temperature and washed 3–5 times with 5% sodium bicarbonate solution until the product was neutral, and then washed 3–5 times with deionized water. Finally, acetylated cyclohexanol ricinolate (ACHR) was purified by partitioning and distillation under reduced pressure.

The refined products, ACHR (422 g, 1 mol) and formic acid (46 g, 0.35 mol), as well as an appropriate amount of ethyl acetate solvent were placed in a three-necked flask, and the temperature was raised to 50 °C after stirring, followed by dropwise addition of hydrogen peroxide (81.6 g, 2.4 mol), which was completed within 30 min. The reaction mixture was heated to 65 °C for 4 h. After the reaction was complete, the refined product, EACHR, was obtained by neutralization and distillation under reduced pressure with water washing. The final yield of the EACHR was 92.8%, and the preparation process is illustrated in Fig. 1.

Synthesis of Epoxyacetyl Ricinoleic Acid Cyclohexanediol Ester (EACHDR)

Synthesis of EACHDR followed the same procedure as that used for EACHR. The only difference lies in the substitution of 1,4-cyclohexanediol for cyclohexanol, which has a carboxyl-to-hydroxyl group ratio of 1.1:1.0. The final yield of EACHDR was 93.2%; the synthetic route is shown in Fig. 2.

Synthesis of Epoxyacetyl Ricinoleic Acid Cyclohexanedimethanol Ester (EACHDMR)

The synthetic route to EACHDMR was analogous to that of EACHDR, except that 1,4-cyclohexanedimethanol was used to replace 1,4-cyclohexanediol. The final yield of EACHDMR was

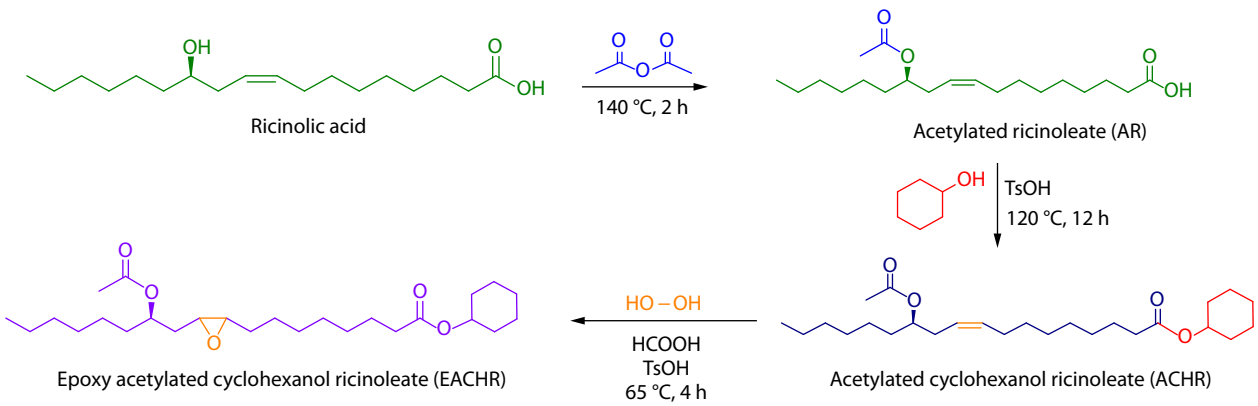

Fig. 1 Synthesis route of epoxyacetyl ricinoleic acid cyclohexanol ester (EACHR).

https://doi.org/10.1007/s10118-026-3698-2

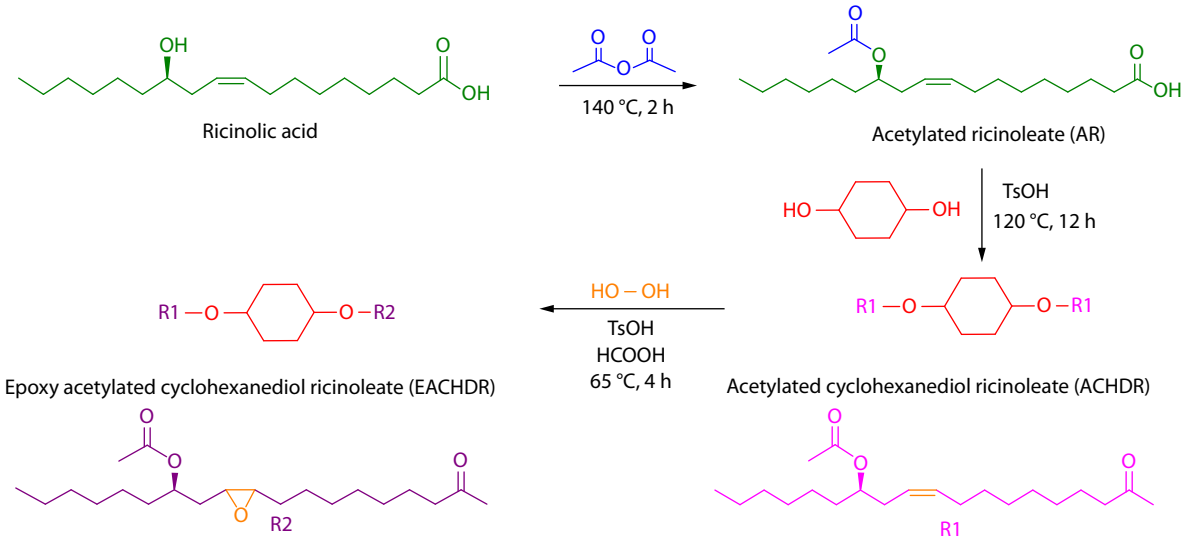

Fig. 2 Synthesis route of epoxyacetyl ricinoleic acid cyclohexanediol ester (EACHDR).

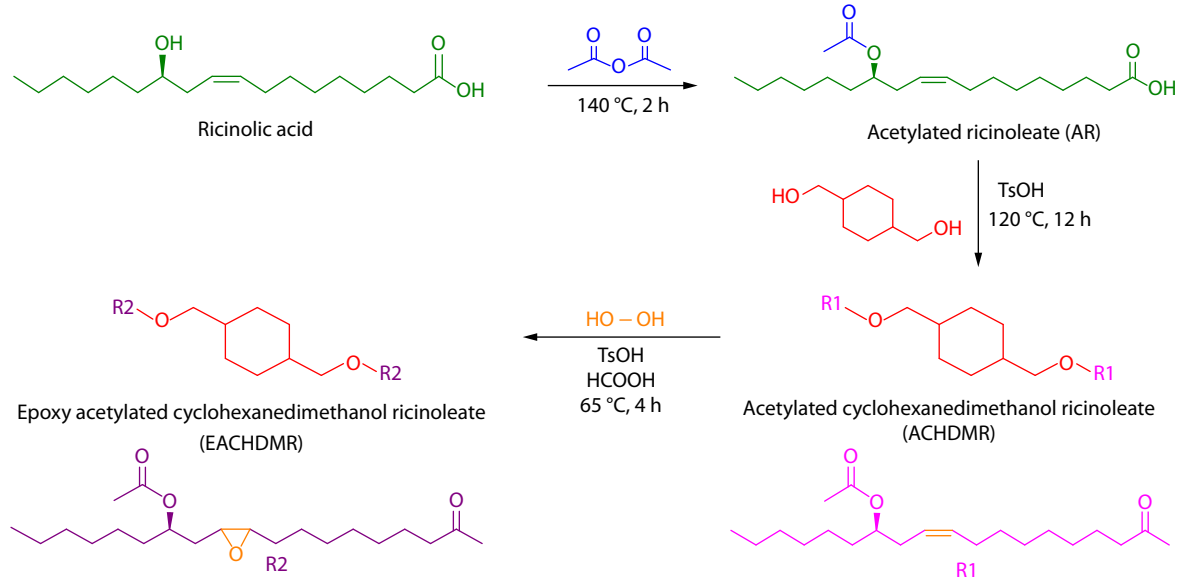

Fig. 3 Synthetic route of epoxyacetyl ricinoleic acid cyclohexanedimethanol ester (EACHDMR).

93.6%; the synthetic route is illustrated in Fig. 3.

Preparation of Plasticized PVC Samples

Prior to processing, poly(vinyl chloride) (PVC) was dried in a vacuum drying oven at 80 °C for a minimum of 8 h to eliminate moisture. Subsequently, castor-oil-based plasticized PVC samples were prepared via melt blending using a two-roll mill. The processing temperature was maintained at 165 °C for 3–5 min. An environmentally friendly methyltin mercaptide (organotin 181) was employed as a processing heat stabilizer. The experimental formulations and sample nomenclature are listed in Table 1.

Characterization

Fourier transform infrared (FTIR) spectroscopy

The chemical structures of the epoxy-functionalized cyclohexane-based ricinoleate plasticizers were confirmed by Fourier transform infrared (FTIR) spectroscopy using a Nicolet IS50 spectrometer. For analysis, each sample was mixed with spectroscopic-grade potassium bromide (KBr) and pressed into pellets. FTIR spectra were recorded in the range of 4000 to 400 cm^{-1} with a resolution of 2 cm^{-1}, averaging 32 scans per spectrum.

Nuclear magnetic resonance (^{1}H-NMR) spectroscopy

^{1}H-NMR spectroscopy was performed on a Bruker Avance III 400 MHz spectrometer. Samples were dissolved in deuterated chloroform ($CDCl_3$) for analysis.

Thermogravimetric analysis (TGA)

The thermal stability of the plasticized PVC samples was evaluated by thermogravimetric analysis (TGA) using a Perkin-Elmer PYRIS-1 TGA instrument. Measurements were performed under a nitrogen atmosphere with sample masses of 8-10 mg, heating from 30 °C to 600 °C at a rate of 10 °C/min.

Mechanical properties

The impact strength was measured using a cantilever beam im-

Table 1 Plasticized PVC sample formulations.

Sample name	PVC	EACHR	EACHDR	EACHDMR	Stabilizer
PVC	100	/	/	/	2
PVC/EACHR10	100	10	/	/	2
PVC/EACHR20	100	20	/	/	2
PVC/EACHR30	100	30		/	2
PVC/EACHDR10	100	/	10	/	2
PVC/EACHDR20	100	/	20	/	2
PVC/EACHDR30	100	/	30	/	2
PVC/EACHDMR10	100	/	/	10	2
PVC/EACHDMR20	100	/	/	20	2
PVC/EACHDMR30	100	/	/	30	2

Note: unit is g, "/" means not added.

pact tester (XJU-22, China), following the GB/T 1843-2008 standard. Tensile tests were performed on an Instron 1121 universal testing machine (USA) at a crosshead speed of 30 mm/min in accordance with GB/T 1040-2018.

Dynamic mechanical analysis (DMA)

Dynamic mechanical analysis (DMA) was conducted on compression-molded specimens (30 mm × 5 mm × 1 mm) using a PerkinElmer Diamond DMA instrument. Tests were performed in tension mode at a frequency of 1 Hz, with temperature ramping from 30 °C to 120 °C at a rate of 3 °C/min.

Shore hardness

The Shore hardness (type D) of the plasticized PVC samples was measured using an LX-D durometer (Shanghai Chuanlu Measuring Instruments Co., Ltd., China), following the ISO 868:2003 standard.

Scanning electron microscope (SEM)

The impact-fractured surfaces of the plasticized PVC samples were examined using a scanning electron microscope (JSM-5600, JEOL, Japan). Prior to observation, all the samples were sputter-coated with gold. The accelerating voltage was maintained between 5 and 10 kV.

Migration and volatility resistance

Migration resistance and volatility resistance tests were conducted in accordance with the ISO 177:1988 (E) standard. The detailed testing procedure is as follows:

(1) Migration resistance test: samples with dimensions of 50 mm × 50 mm ×1 mm were prepared using a hot-pressing method. The initial mass M_0 was recorded. The samples were subjected to leaching experiments in deionized water and n-hexane at 30 °C for 48 h. Subsequently, the liquid on the sample surface was rinsed off and the samples were dried before measuring the final mass, M_1.

(2) Volatility resistance test: samples with dimensions of 50 mm × 50 mm × 1 mm were prepared, and the initial mass, M_0, was recorded. The samples were then placed in an oven at 70 °C for 24 h, and the mass, M_1, was measured after the test.

The migration and volatility resistance of the plasticizer in the samples were evaluated based on the mass loss ratio (V) calculated using Eq. (1).

$$V = \frac{M_0 - M_1}{M_0} \quad (1)$$

Analysis of plasticizing efficiency

To further compare the effects of plasticizers, a series of PVC samples containing equal molar amounts of plasticizers was tested on compression-molded specimens (30 mm × 5 mm × 1 mm) using a PerkinElmer Diamond DMA. Tests were performed in tension mode at a frequency of 1 Hz, with temperature ramping from 30 °C to 120 °C at a rate of 3 °C/min. The T_g reduction range of T_g was determined by DMA, and the plasticizing efficiency of each plasticizer was quantitatively evaluated.

This study employs two evaluation systems. The equal-mass loading system (10 wt%, 20 wt%, and 30 wt%) simulated the actual industrial application scenario and was used to evaluate the comprehensive performance (mechanical properties, thermal stability, resistance to migration and volatility, and yellowing index). The equal-mole loading system (Table 2) was used to compare the intrinsic plasticizing efficiency of different plasticizer molecules on a fair basis, based on the reduction in the glass transition temperature.

Yellowing index

The inhibitory effects of different plasticizers on the dechlorination of PVC were evaluated through a thermal aging experiment. The plasticized PVC samples were cut into square thin sheets, placed in a forced-air oven, and subjected to constant temperature aging at 120 °C. Samples were taken out at aging times of 0, 10, 50, 90, 170, and 190 min and rapidly cooled to room temperature. The b^* value (yellow-blue value) of the samples was measured in the CIE Lab color space using a colorimeter (CR-10plus, KONLCA MINOLTA). The b^*_{before} value is used to measure the degree of yellowing before aging. The b^*_{after} is used to measure the degree of yellowing after aging. At least three measurements were performed for each sample, and the aver-

Table 2 Two evaluation frameworks for plasticization performance.

System	Key parameter	EACHDMR versus DOTP
Equal-mass (10 wt%–30 wt%)	Mechanical properties; Thermal stability; Migration/volatility resistance; T_g reduction; Yellowing index	Comparable or superior
Equimolar	Relative plasticization efficiency	120.7% (20.73% higher)

https://doi.org/10.1007/s10118-026-3698-2

age value was calculated. The yellowing index (Δb^*) was calculated using the following Eq. (2):

$$\Delta b^* = b^*_{\text{before}} - b^*_{\text{after}} \quad (2)$$

RESULTS AND DISCUSSION

FTIR

The chemical structures of the synthesized epoxy-functionalized cyclohexanecarboxylate plasticizers (EACHR, EACHDR, and EACHDMR) were confirmed using Fourier transform infrared (FTIR) spectroscopy. As shown in Fig. 4, the FTIR spectra exhibited characteristic absorption bands that were aligned with the designed molecular features. The consumption of ricinoleic acid was indicated by the disappearance of its broad hydroxyl (O—H) stretching band at approximately 3400 cm^{-1}. Meanwhile, Successful acetylation and esterification were confirmed by the appearance of a strong carbonyl (C=O) stretching vibration at approximately 1740 cm^{-1} and the associated C—O—C stretching bands at 1240 and 1150 cm^{-1}. Critically, the presence of the absorption band at 910 cm^{-1}, characteristic of the epoxy group, verifies the introduction of this key polar functionality. Collectively, these spectral features validated the successful execution of the synthetic route, yielding target compounds with the intended functional groups.

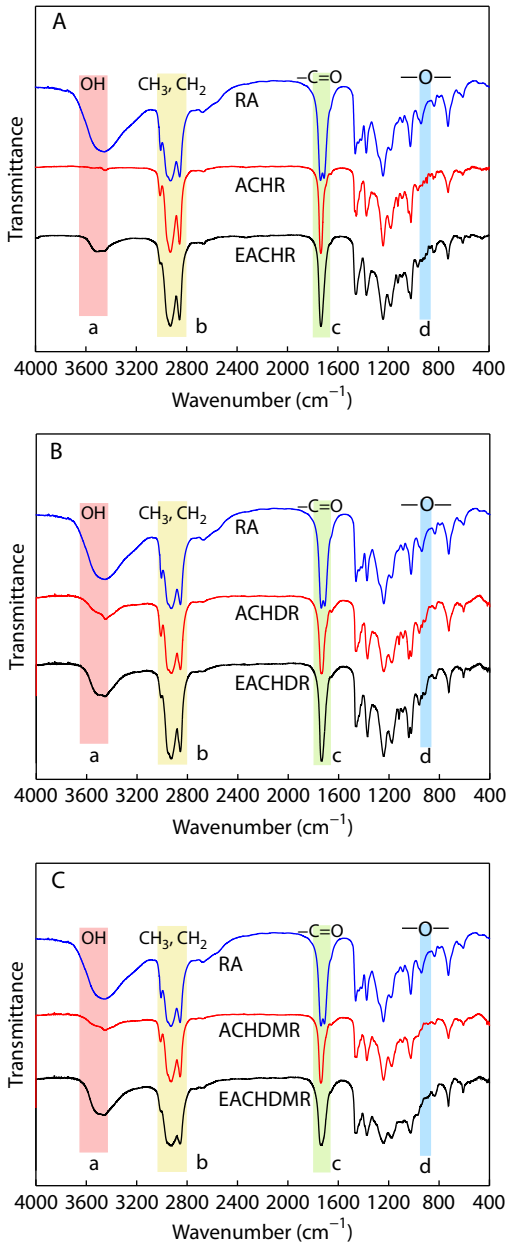

Fig. 4 FTIR spectra of (A) EACHR, (B) EACHDR, (C) EACHDMR.

^{1}H-NMR

The molecular structures of EACHR, EACHDR, and EACHDMR were confirmed using ^{1}H-NMR spectroscopy showed in Fig. 5. The observed signals in the spectra are consistent with the expected epoxy-functionalized cyclohexanecarboxylate structure. The terminal methyl protons (signal a) at δ=0.88 ppm; the complex set of signals from aliphatic methylene protons (signal b) in the broad envelope of δ=1.2–1.8 ppm, originating from both the fatty acid chain and the cyclohexyl ring. The acetyl methyl protons (contributing to signal c) resonated around δ=2.0–2.1 ppm, while protons adjacent to the carbonyl and epoxy groups (signal d) were observed at δ=2.27–2.28 ppm. The protons in the critical linker region between the ester and cyclohexyl rings gave rise to distinct patterns. For EACHR, the methylene protons (O—CH_2, signal e) appeared as characteristic multiplets between δ=4.7 and 4.9 ppm. In contrast, for the symmetric derivatives EACHDR and EACHDMR, the corresponding methine or methylene protons in this region (signal e) produced a different, specific pattern between δ=4.8 and 4.9, consistent with their para-disubstituted cyclohexane structures. The diagnostic methine proton on the acetylated ricinoleate backbone (signal f) was clearly observed as a multiplet in the region δ=5.3–5.5 ppm. The integration values derived from the spectra (Table 3) are in good agreement with the theoretical proton counts for each target molecule. The overall spectral purity was high, and there was very little stray resonance, which guaranteed the successful formation of the target compound.

Thermal Stability

As shown in Fig. 6, the PVC sample exhibited a two-phase breakdown mechanism. The temperature range for the first stage is 260–370 °C. This is primarily attributed to the thermal decomposition of the plasticizer and dehydrochlorination of the PVC matrix.[32,33] The temperature range for the second phase was between 450 and 530 °C, which is primarily attributed to the structural rearrangement of the PVC macromolecules and cleavage of the carbon skeleton.[34] The temperature at which the plasticized PVC sample lost 5% of its mass was recorded as $T_{5\%}$. It can be used to analyze the influence of plasticizers on the first-stage dechlorination decomposition behavior of poly(vinyl chloride) or volatilization of plasticizers. Compared to neat PVC, the addition of plasticizers improved the thermal stability of PVC. As shown in Table 4, the initial decomposition temperature ($T_{5\%}$) increased. Specifically, EACHDMR demonstrated excellent thermal stability. For instance, the $T_{5\%}$ of PVC/EACHDMR30 (282.4 °C) was higher than that of PVC/DOTP30 (250.9 °C), suggesting that DOTP-plasticized PVC undergoes earlier volatilization or initial dehydrochlorination. This was further confirmed by the DTG curve: PVC/DOTP30 showed a more pronounced peak in the first degradation stage,

https://doi.org/10.1007/s10118-026-3698-2

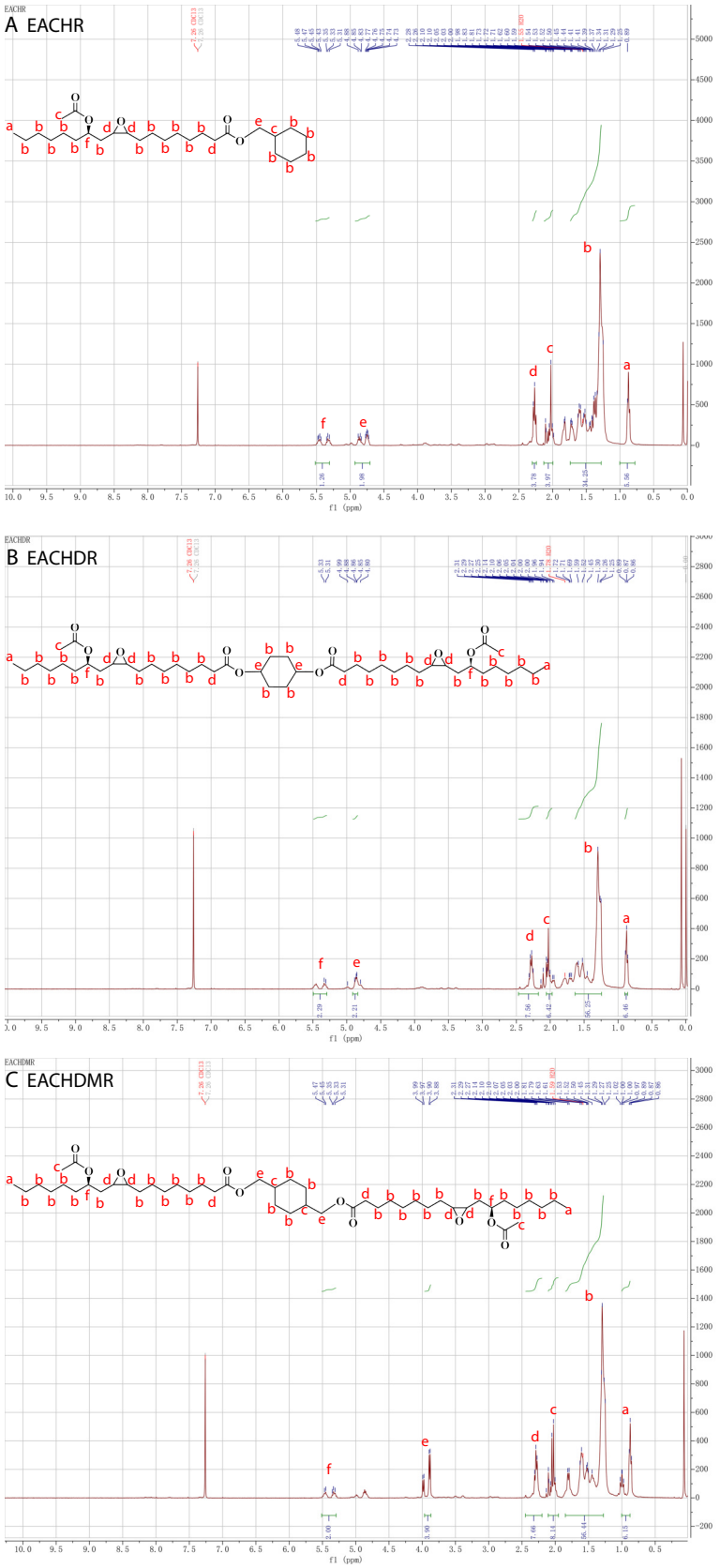

Fig. 5 ^{1}H-NMR spectra of plasticizers (A) EACHR, (B) EACHDR, (C) EACHDMR.

https://doi.org/10.1007/s10118-026-3698-2

Table 3 ^{1}H-NMR spectra data of EACHR, EACHDR, and EACHDMR.

Plasticizer	^{1}H-NMR（400 MHz: CDCl3, δ, ppm, J in Hz）
EACHR	^{1}H-NMR (400 MHz, Chloroform-d, δ, ppm): 5.52–5.31 (m, 1H), 4.93–4.71 (m, 2H), 2.27 (d, J=7.5 Hz, 4H), 2.13–2.00 (m, 4H), 1.74–1.28 (m, 34H), 0.89 (s, 6H).
EACHDR	^{1}H-NMR (400 MHz, Chloroform-d, δ, ppm): 5.32 (d, J=9.7 Hz, 2H), 4.91–4.84 (m, 2H), 2.28 (q, J=8.1 Hz, 8H), 2.06–1.97 (m, 6H), 1.63–1.24 (m, 56H), 0.88 (d, J=6.1 Hz, 6H).
EACHDMR	^{1}H-NMR (400 MHz, Chloroform-d, δ, ppm): 5.51–5.30 (m, 2H), 3.89 (d, J=6.5 Hz, 4H), 2.29 (t, J=7.6 Hz, 8H), 2.11–1.95 (m, 8H), 1.85–1.28 (m, 56H), 1.00–0.88 (m, 6H)

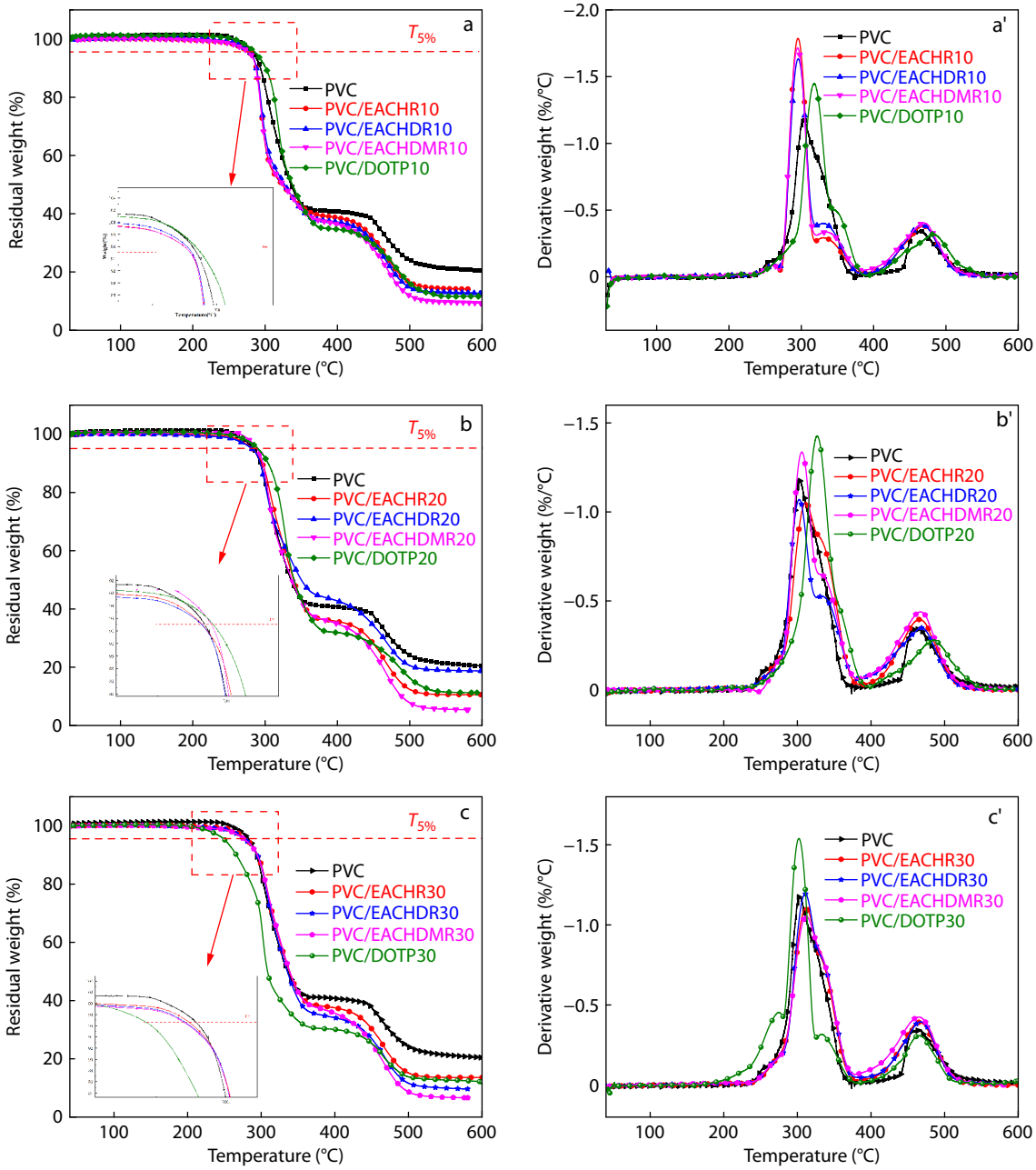

Fig. 6 TGA (a, 10 wt%; b, 20 wt%; c, 30 wt%) and DTG (a′, 10 wt%; b′,20 wt%, c′,30 wt%) curves of plasticized PVC samples.

accompanied by a low-temperature shoulder, whereas PVC/EACHDMR30 exhibited a relatively wide peak and its position shifted to a higher temperature. Residual mass was quantified at 400 °C. At 400 °C, the residual mass of PVC/EACHDMR30 was 35.65%, whereas that of PVC/DOTP30 was 30.05%, (Table 4) which confirmed that it had better thermal stability in the early stage.

This was also confirmed by comparing the maximum thermal decomposition temperatures (T_{max}) of the plasticized samples. PVC/EACHDMR had a T_{max} that was comparable to

that of PVC/DOTP and higher than those of PVC/EACHR and PVC/EACHDR. Specifically, PVC/EACHDMR30 exhibited a T_{max} (313.1 °C) superior to that of PVC/DOTP30 (302.5 °C). This enhancement can be attributed to the synergistic molecular design of the EACHDMR. Specifically, its polar epoxy and ester groups can interact with the active chlorine atoms in PVC, thereby potentially inhibiting autocatalytic dechlorination.[35,36] Meanwhile, its rigid cyclohexane ring provides steric hindrance and thermal stability similar to that of the benzene ring in DOTP.[37]

By analyzing the two-stage degradation behavior of the PVC plasticization samples, it was found that the addition of plasticizers reduced the two-stage decomposition of PVC and improved its thermal stability. Specifically, in the plasticized sample with 10 wt% plasticizer content, the synthesized samples showed a quality residue similar to that of PVC/DOTP; for example, at 500 °C, the quality residue of PVC/DOTP10 was 16.06%, while the quality residues of PVC/EACHR10, PVC/EACHDR10, and PVC/EACHDMR10 were 16.45%, 14.68%, and 11.86%, respectively. This indicates that ricinoleic acid-based plasticizers, owing to their alkyl cyclic structure, more abundant ester and epoxy groups, and relative molecular mass, can reduce the degree of two-stage decomposition of PVC plasticized samples, thereby achieving thermal stability similar to that of DOTP in the two-stage decomposition of PVC.

Mechanical Properties

By examining the static and dynamic mechanical properties of polymers, the influence of plasticizers on their ductility and flexibility can be comprehensively evaluated.[38] Fig. 7(a) shows that the notched impact strength of neat PVC is only 28 J/m, which is typical for brittle materials.[39] After the addition of the bio-based plasticizers, the performance was significantly enhanced. Specifically, the notched impact strengths of PVC/EACHR20 and PVC/EACHDMR20 were 1280 and 1024 J/m, respectively. These values surpassed those of neat PVC, but their performance was comparable to or even better than that of PVC/DOTP20. This toughening effect stems from the intermolecular synergistic design: its polar epoxy and ester groups interact with the PVC chain, weakening the intermolecular forces. The rigid cyclohexane ring introduced a significant free volume. This combination promoted chain slip and energy dissipation under impact, simulating the stereoscopic hindrance effect of the benzene ring in DOTP.[40] In contrast, at the same addition amount, the notched impact strength performance of the EACHDR was significantly inferior.

As shown in Figs. 7(b)–7(d) and Table 5, the tensile tests further clarified the plasticizing effect. With an increase in the plasticizer content, the elongation at break significantly increased, whereas the modulus correspondingly decreased. For instance, the elongation at break of PVC/EACHR20 and PVC/EACHR30 reached 158.81% and 208.99%, respectively, whereas that of neat PVC was only 3.1%. Correspondingly, the modulus decreased to 548 and 148 MPa. Under other test contents, the tensile properties of EACHR and EACHDMR were comparable to those of DOTP, confirming their effectiveness as plasticizers. In contrast, EACHDR performed poorly in terms of elongation at break and modulus.

The relatively poor mechanical properties of EACHDR deserve attention. Its symmetrical molecular structure may lead to a decrease in the efficiency of the intermolecular interactions. Meanwhile, the free volume produced in the PVC matrix was not as high as that produced by EACHR and EACHDMR. When the addition amount reached 30%, this led to an excessive reduction in the modulus, as shown in the tensile data. Although enhanced chain fluidity can increase the elongation at break of materials, an excessively low modulus weakens the ability of the material to effectively absorb and disperse impact energy, which is associated with the observed reduction in notched impact strength.[41] This indicates that achieving the best plasticization requires a balance between the flexibility and rigidity.

The performance of EACHR and EACHDMR verified the core design hypothesis that aliphatic cyclohexane rings can effectively replace benzene rings as rigid cores. Under the same test conditions, the data for plasticizers containing benzene rings with similar structures (EABR and EATPR) were compared, further confirming this conclusion.[42] The impact strength of PVC/EACHR20 (1280 J/m) is considerably higher than that of PVC/EABR20 (465 J/m). Similarly, PVC/EACHDMR20 (1084 J/m) matches the performance of PVC/EATPR20 (1072 J/m). These comparisons provide evidence that sustainable cyclohexane-based designs can match and even surpass the effectiveness of traditional aromatic structures for enhancing the mechanical strength of PVC.

Table 4 Thermal parameters of plasticizers and plasticized PVC samples.

Sample	$T_{5\%}$ (°C)	T_{max} (°C)	Residual mass (%)		
			400 °C	500 °C	600 °C
PVC	284.3	298.3	40.76	24.16	20.46
PVC/DOTP10	287.3	317.9	34.65	16.06	11.66
PVC/DOTP20	288.6	326.8	31.86	16.34	11.26
PVC/DOTP30	250.9	302.5	30.05	13.82	12.07
PVC/EACHR10	279.6	296.8	38.63	16.45	14.14
PVC/EACHR20	282.2	310.3	35.71	12.36	10.57
PVC/EACHR30	281.4	311.9	37.51	15.17	13.61
PVC/EACHDR10	280.6	294.8	37.15	14.68	12.64
PVC/EACHDR20	281.9	303.1	42.76	20.61	18.72
PVC/EACHDR30	279.8	310.2	34.12	11.66	9.66
PVC/EACHDMR10	281.1	300.4	36.37	11.86	9.21
PVC/EACHDMR20	289.1	306.2	34.94	7.76	5.41
PVC/EACHDMR30	282.4	313.1	35.65	8.68	6.65

https://doi.org/10.1007/s10118-026-3698-2

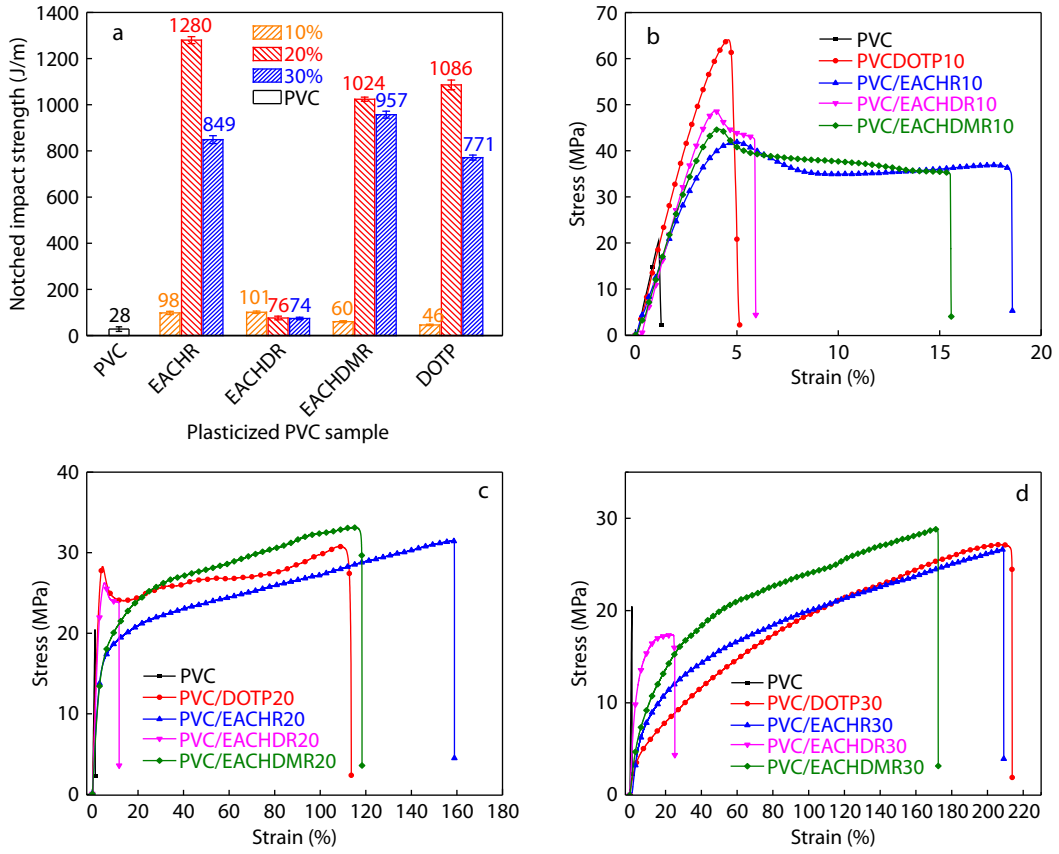

Fig. 7 Mechanical properties of plasticized PVC samples: (a) notched impact strength, (b) stress-strain curves of 10 wt%, (c) stress-strain curves of 20 wt%, and (d) stress-strain curves of 30 wt%.

Table 5 Notched impact and tensile properties of neat PVC and plasticized PVC samples.

Sample name	Notched impact strength (J/m)	Tensile strength at break (MPa)	Elongation at break (%)	Young's modulus (MPa)
PVC	28±2	39.6±2.1	3.2±1.1	1768±11
PVC/EACHR10	98±7	35.62±2.4	18.48±0.7	1479±13
PVC/EACHR20	1280±15	31.41±0.41	158.81±3.2	538±8
PVC/EACHR30	849±17	26.6±1.51	208.99±4.2	148±5
PVC/EACHDR10	101±5	37.19±2.3	5.82±2.1	1652±11
PVC/EACHDR20	76±8	26.81±2.8	11.62±4.2	856±9
PVC/EACHDR30	74±5	20.41±1.9	25.06±4.81	341±14
PVC/EACHDMR10	60±4	35.41±3.4	15.46±2.5	1535±21
PVC/EACHDMR20	1024±9	29.44±3.1	118.23±6.3	596±12
PVC/EACHDMR30	957±15	26.69±1.4	172.36±3.3	142±4
PVC/DOTP10	46±3	42.6±2.2	4.8±1.5	1788±13
PVC/DOTP20	1086±21	20.2±0.8	113.2±5.6	1115±56
PVC/DOTP30	771±11	25.7±3.5	214.1±8.5	58±12

Dynamic Mechanical Analysis

The plasticizing effect is further quantified through dynamic mechanical analysis (DMA). The reduction in the glass transition temperature (T_g) is a key indicator for measuring the performance of plasticizers.[43] As shown in Fig. 8, with an increase in plasticizer content, the T_g of the PVC sample gradually decreased. For instance, the T_g values of PVC/EACHR10, PVC/EACHR20, and PVC/EACHR30 are 69.17, 57.47, and 48.75 °C, respectively, which are significantly lower than those of neat PVC at 30 wt% by 39.28 °C. This trend confirms that the plasticizers efficiently disrupted the dipole-dipole interactions between the PVC chains, increasing the chain mobility.

A comparative analysis revealed distinct structure-performance trends. At 30 wt%, both EACHR and EACHDMR could effectively reduce T_g to 48.75 and 55.97 °C, respectively, which was comparable to or lower than the T_g value of 53.37 °C for PVC/DOTP. In contrast, EACHDR induced a notably smaller reduction in T_g levels. This might be because the asymmetric single-ring structure of EACHR and the symmetrical double-substituted ring structure of EACHDMR provide greater steric hindrance, thereby effectively increasing the free volume between the PVC chains. Although the molecu-

https://doi.org/10.1007/s10118-026-3698-2

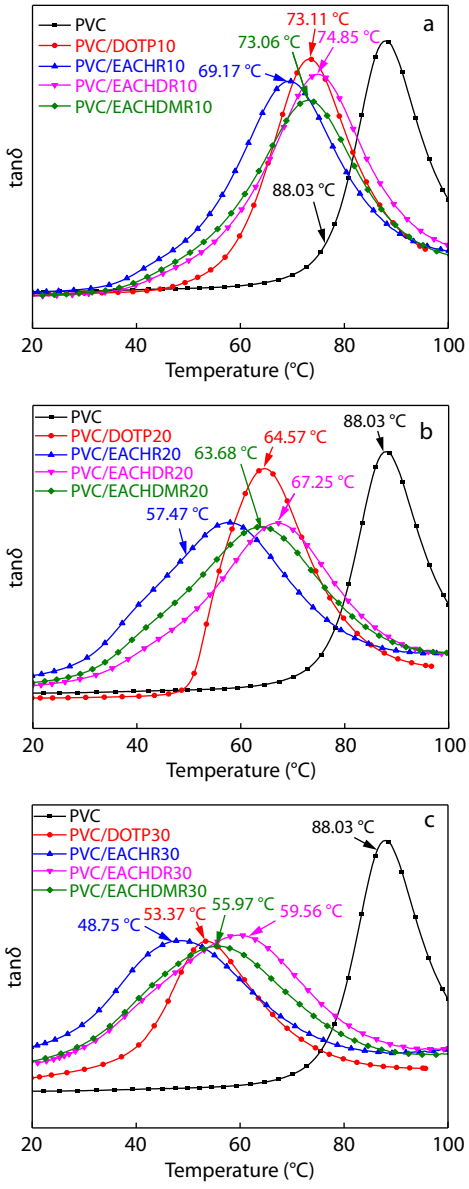

Fig. 8 DMA curves of plasticized PVC samples. (a) 10 wt%; (b) 20 wt% and (c) 30 wt%.

lar weights of EACHDMR and EACHDR are similar, the former performs better, highlighting the significance of the molecular geometry and the presence of flexible methylene spacers in the cyclic substituents in achieving optimal compatibility and plasticizing efficiency.

The single tanδ peaks observed for the blends indicate the absence of macroscopic phase separation between the plasticizers and PVC matrix.[44] However, EACHDR has a poor effect on reducing T_g and its mechanical properties, revealing a key difference in its plasticizing efficiency. This demonstrates that while EACHDR achieves a molecular-level dispersion sufficient to prevent a separate thermal transition, its specific symmetric molecular structure affords less effective disruption of PVC chain-chain interactions compared to EACHR and EACHDMR. This low plasticizing efficiency indicates that the EACHDR may approach its actual compatibility limit at lower effective concentrations. This hypothesis was further confirmed using SEM.

Shore Hardness

Testing the hardness of the plasticized sample can characterize the plasticizing effect of the plasticizer. As shown in Fig. 9, the hardness of the plasticized PVC samples gradually decreased with an increase in the plasticizer content. For example, the hardness of neat PVC (58) was reduced to 50 for PVC/EACHR10, 45 for PVC/EACHR20, and 40 for PVC/EACHR30. A comparative analysis at 30 wt% established the following performance order: PVC/EACHR30 < PVC/EACHDMR30 < PVC/DOTP30 < PVC/EACHDR30. These results indicate that EACHR and EACHDMR had significant softening effects on PVC. Its plasticizing performance is comparable to or even surpasses that of DOTP. In contrast, PVC/EACHDR30 demonstrated the highest hardness among the plasticized samples, reflecting its relatively weak ability to break the rigidity of the PVC matrix. This result shows a correlation with mechanical data. Although PVC/EACHDR30 had a relatively good rigidity retention capacity, its impact strength and elongation at break were relatively low. This indicates that its compatibility with PVC is limited and the intermolecular interaction efficiency is relatively low. It not only fails to provide an effective toughening effect, but also leads to plasticized PVC samples being both brittle and not fully softened. The effects of EACHR and EACHDMR on hardness reduction confirmed their successful molecular design.

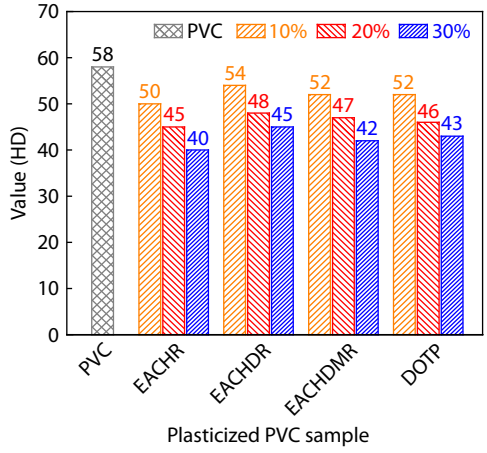

Fig. 9 Shore hardness of plasticized PVC samples D.

Microscopic Morphology Analysis

As shown in Fig. 10(a), with an increase in plasticizer content, the impact fracture morphology of the plasticized PVC sample changed significantly. The cross-section was relatively smooth, with only a few stress whitening points appearing in some samples with low plasticizer concentrations. In contrast, at higher plasticizer concentrations, the overall morphology became significantly rougher and more irregular. This micro-morphological change reflects the transformation of the material from brittle to ductile, indicating enhanced plasticity, especially in the EACHR and EACHDMR samples.

Conversely, the fracture surface of PVC/EACHDR exhibited the least change. It maintains a relatively flat and featureless structure even at a high plasticizer content. The density of the stress-whitening points was significantly lower, and evidence

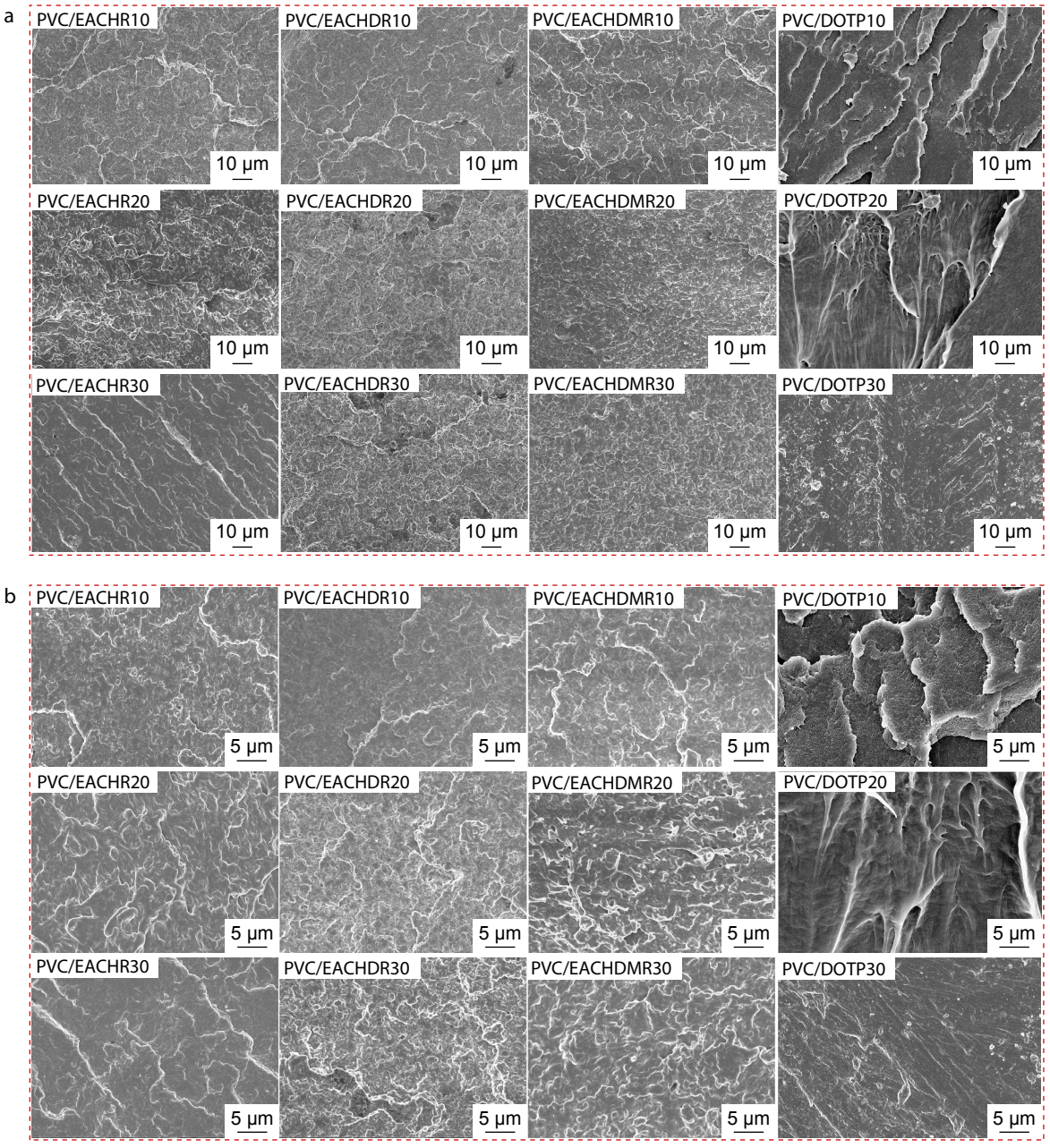

Fig. 10 SEM photographs of plasticized PVC samples. (a) 1000x; (b) 3000x.

of tearing or plastic deformation was scarcely observed, consistent with its inferior impact toughness. The high-magnification image Fig. 10(b) further reveals that PVC/EACHDR has pores and inhomogeneous structures, especially at high concentrations, which indicates that the plasticizer has undergone agglomeration and microphase separation. This observation provides a direct microstructural explanation for the poor mechanical and migration properties of PVC/EACHDR. In comparison, the fracture surfaces of PVC/EACHR30, PVC/EACHDMR30, and PVC/DOTP30 were uniformly rough and densely textured with no obvious signs of phase separation. This morphology confirms that EACHR and EACHDMR have good compatibility and stable dispersion in the PVC matrix, which is consistent with their relatively good overall performance.

Migration and Volatility Resistance

In addition to enhancing the mechanical and thermal properties, plasticized PVC should possess long-term stability and safety. This requires excellent resistance to plasticizer migration and volatility. The corresponding data can be obtained by calculating according to Eq. (1). As shown in Figs. 11(a) and 11(b) and Table 6, the migration resistance of all plasticizers decreased with an increase in the plasticizer content. This might be due to an increase in concentration. At 30 wt%, EACHDMR exhibited the lowest mass loss in both solvents, demonstrating a relatively high migration resistance. EACHR exhibited a similar migration performance to DOTP in deionized water, but at a loading of 30 wt%, the mass loss in *n*-hexane was slightly higher. Mean-

https://doi.org/10.1007/s10118-026-3698-2

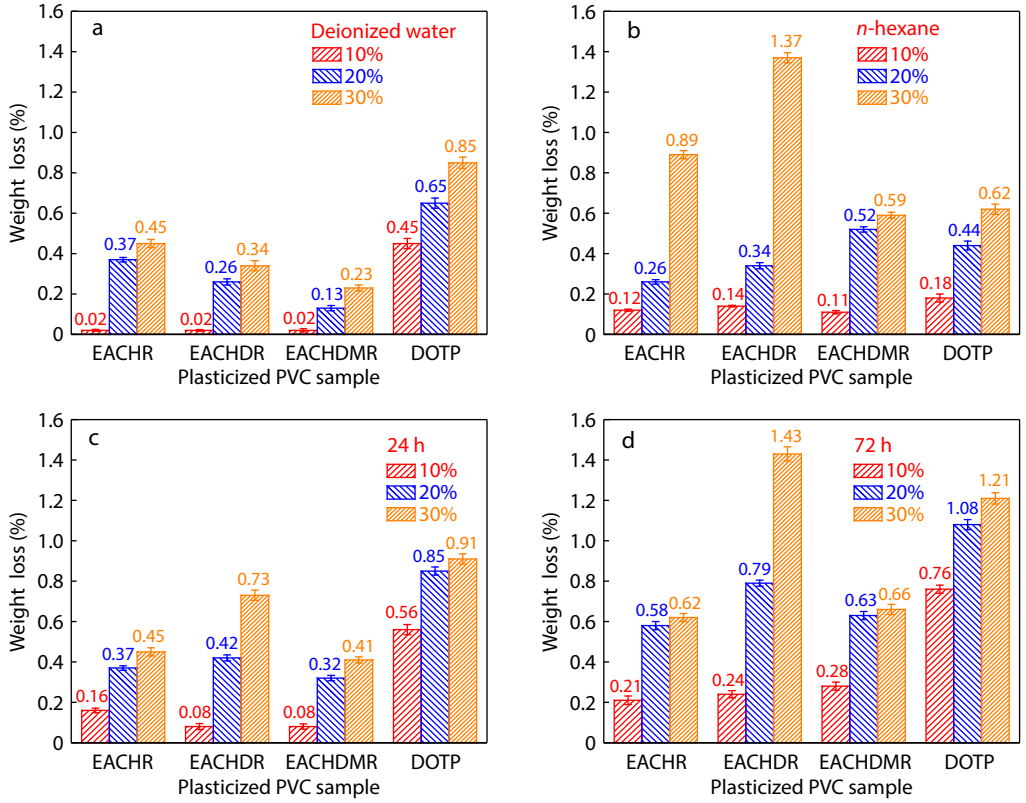

Fig. 11 Test results of migration and volatility tests: (a) in deionized water; (b) in *n*-hexane; (c) in 24 h; (d) in 72 h.

Table 6 Migration and volatility test data of plasticized PVC samples.

Mass loss Sample	Hexane 48 h	Deionized water 48 h	Volatility resistance	
			24 h	72 h
PVC/DOTP10	0.18	0.45	0.56	0.76
PVC/DOTP20	0.44	0.65	0.85	1.08
PVC/DOTP30	0.62	0.85	0.91	1.21
PVC/EACHR10	0.12	0.02	0.16	0.21
PVC/EACHR20	0.26	0.37	0.37	0.58
PVC/EACHR30	0.89	0.26	0.45	0.62
PVC/EACHDR10	0.14	0.02	0.08	0.24
PVC/EACHDR20	0.34	0.26	0.42	0.79
PVC/EACHDR30	1.37	0.34	0.73	1.43
PVC/EACHDMR10	0.11	0.02	0.08	0.28
PVC/EACHDMR20	0.52	0.13	0.32	0.63
PVC/EACHDMR30	0.59	0.23	0.41	0.66

while, the migration rate of the EACHDR was always the highest in deionized water. Notably, the migration behavior of the plasticizers also showed a significant solvent dependence. Under the same conditions, the same plasticizer exhibits different migration rates in different solvents, which can be explained by the principle of "like dissolves like" and the solvation parameter theory: the long alkyl chain part of *n*-hexane (solubility parameter: 14.9 $MPa^{1/2}$)[45] has better affinity with the plasticizer molecules, making it easier to extract free plasticizer molecules, while polar water molecules (solubility parameter: 47.9 $MPa^{1/2}$)[46] have poor compatibility with the plasticizer and the hydrophobic PVC matrix, so the extraction effect is weaker. Under the same solvent conditions, this result may not be explained solely by the molecular weight, as EACHDMR and EACHDR have similar molecular weights. Instead, molecular structure plays a decisive role. The large and symmetrical structure of EACHDMR provides a greater steric hindrance effect and may have better compatibility with PVC, thereby effectively anchoring molecules in the polymer matrix. In contrast, the linear vicinal diol structure of EACHDR may lead to poorer compatibility and thus higher mobility, consistent with its performance in mechanical tests.

Similarly, in the volatility test (Figs. 11c and 11d), the performance of all synthesized plasticizers was superior to that of DOTP. Among them, EACHDMR had the lowest mass loss (0.41%) after 24-h testing at 70 °C, whereas the mass loss of PVC/DOTP30 reached 0.91%. The EACHR and EACHDMR performed better than the EACHDR. Although a higher molecu-

Table 7 Formulations for plasticized PVC samples (molar amount of plasticizer 0.01mol).

Sample Name	PVC	EACHR	EACHDR	EACHDMR	Stabilizer
PVC/mDOTP	100	/	/	/	2
PVC/mEACHR	100	4.38	/	/	2
PVC/mEACHDR	100	/	7.78	/	2
PVC/mEACHDMR	100	/	/	8.06	2

Note: Unit g, "/" means not added.

lar weight usually indicates lower volatility, when the molecular weights are similar, EACHDMR performs better than EACHDR, further highlighting the importance of molecular design. In summary, EACHDMR demonstrated outstanding and comprehensive durability, exhibiting significantly lower migration and volatility than the commercial benchmark DOTP. Its performance surpasses that of the structural analogs EACHR and EACHDR. Its outstanding stability is directly attributed to the "flexible-rigid-polar" molecular design, especially the effective application of cyclohexanedimethanol-derived aliphatic rings.

Analysis of Plasticizing Efficiency

To further compare the effects of plasticizers, a series of PVC samples containing equal molar amounts of plasticizers was prepared in this study (Table 7). The T_g reduction range of T_g was determined by DMA, and the plasticizing efficiency of each plasticizer was quantitatively evaluated (Fig. 12).

The glass transition temperature (T_g) shows a clear order (Table 8): PVC/mEACHDMR(73.88 °C)<PVC/mEACHDR(75.16 °C)<PVC/mDOTP(76.31 °C)≈PVC/mEACHR(76.38 °C). The relative plasticizing efficiency was calculated based on DOTP (100%) Eq. (3). EACHR showed comparable efficiency (99.41%), whereas EACHDR and EACHDMR exhibited superior efficiencies of 109.81% and 120.73%, respectively, outperforming DOTP at 9.81% and 20.73%, respectively.

$$E_{\Delta Tg(\%)} = \frac{\Delta T_g}{\Delta T_{g,DOTP}} \times 100\% \quad (3)$$

This performance may be attributed to molecular design. Although both EACHDR and EACHDMR are symmetrical structures containing polar groups, the cyclohexane substituent in EACHDMR has a methylene spacer group. This structure endows the molecular chain with higher conformational degrees of freedom and movement capabilities, thereby more effectively inserting into the PVC chain and enhancing plasticizing efficiency.

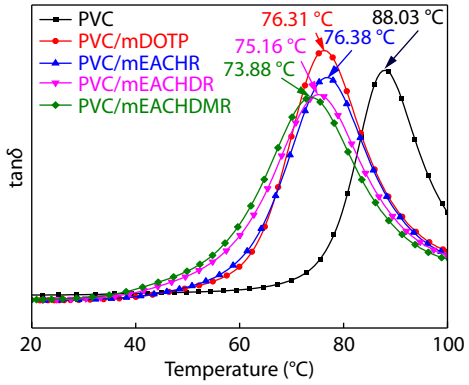

Fig. 12 DMA curves of PVC samples plasticized with equimolar plasticizer content.

Table 8 Analysis of plasticizing efficiency data for plasticized samples (equimolar amount).

Sample	T_g (°C)	ΔT_g (°C)	$E_{\Delta Tg}$ (%)
PVC	88.03	0	/
PVC/mDOTP	76.31	11.72	100.00
PVC/mEACHR	76.38	11.65	99.41
PVC/mEACHDR	75.16	12.87	109.81
PVC/mEACHDMR	73.88	14.15	120.73

Yellowing Index

To directly assess the ability of the synthesized plasticizers to inhibit the dehydrochlorination reaction of PVC, the yellowing index (Δb^*) was measured for all the samples after they were thermally aged at 120 °C for a certain period of time, as shown in Fig. 13.[47,48] The unplasticized PVC exhibited the most severe color change, with Δb^* reaching 12.3 after 190 min of aging, which was due to the rapid formation of conjugated diene sequences through the self-catalytic dehydrochlorination reaction. In contrast, the Δb^* values of all the plasticized samples were significantly reduced, confirming the stabilizing effect of the plasticizers. As shown in Fig. 13, pure PVC exhibited evident yellowing within 50 min before aging, indicating that the dehydrochlorination reaction was initiated rapidly. After adding plasticizers, the yellowing phenomenon of the composite materials was alleviated to varying degrees, with the sample containing 10 wt% DOTP showing a relatively weaker inhibitory effect. When the plasticizer mass fraction was 10%, the EACHDMR-plasticized samples showed the lowest Δb^* values at all time points, indicating a strong inhibitory effect on dehydrochlorination. This result may be attributed to the interaction between the epoxy groups in the EACHDMR molecule and the active chlorine atoms on the PVC chain, which effectively delays dehydrochlorination.

As the mass fraction of the plasticizer increased from 10% to 30%, the Δb^* value of each sample showed an overall downward trend, indicating that the increase in plasticizer concentration further enhanced the inhibitory effect on the dehydrogenation of hydrogen chloride, demonstrating a clear dose-dependent relationship. At a fixed aging time point of 190 min, the yellowing of pure PVC was the most severe, and in the early stage of 50 min, the samples with EACHDMR plasticization showed significantly lower Δb^* values than the other samples, proving that it could exert an effective inhibitory effect in the early stage of aging. This early inhibitory behavior is consistent with the observation of reduced early mass loss in thermogravimetric analysis, further verifying the chemical stability of the epoxy groups against the dehydrogenation of hydrogen chloride.

Structure-property Relationships and Design Principles

The above data show a comprehensive performance sequence of EACHDMR>EACHR>EACHDR. This may be attributed to the

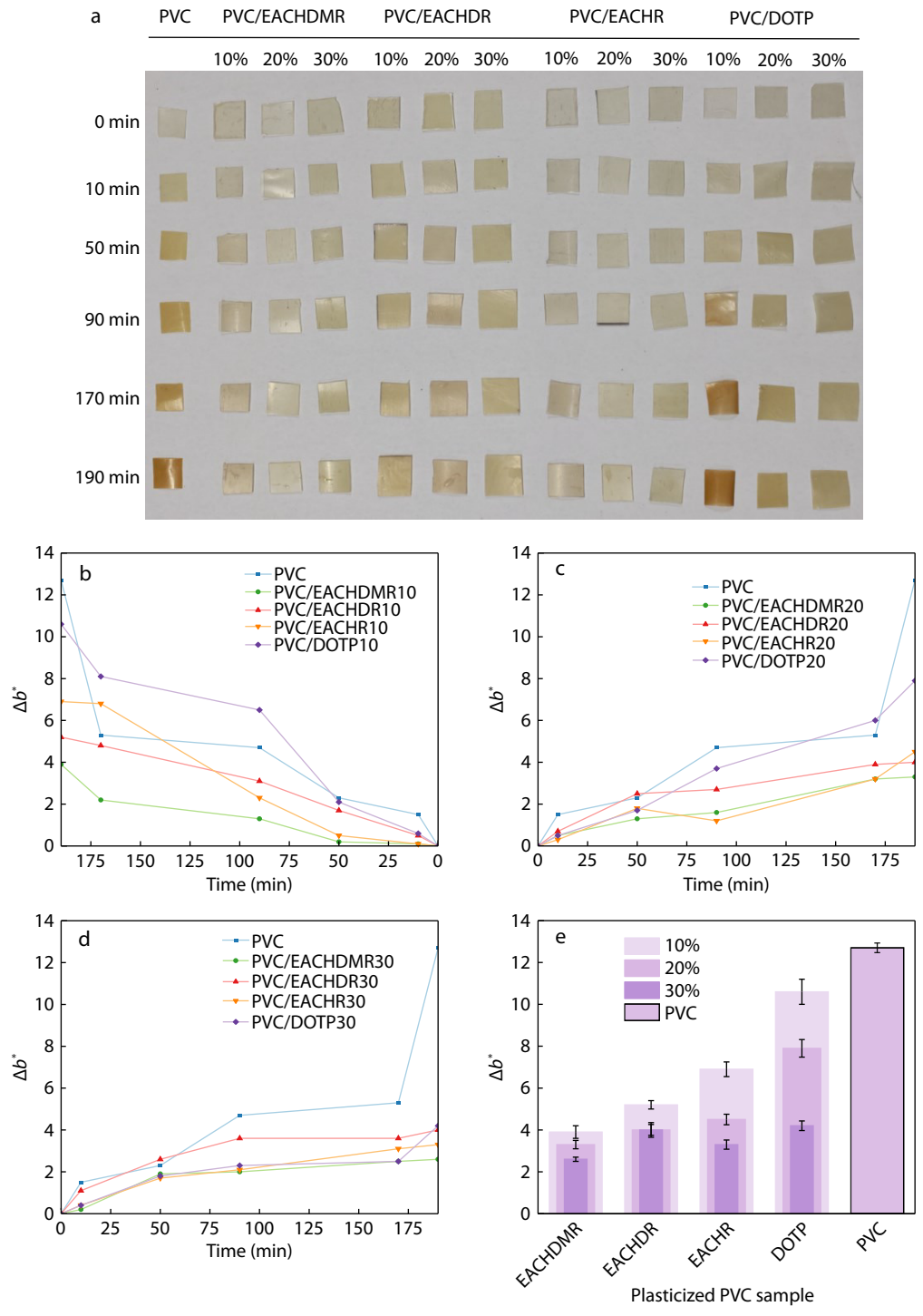

Fig. 13 Thermal aging behavior of pure PVC and plasticized PVC samples at 120 °C. (a) Optical images of samples taken at different time intervals; (b–d) Δb^* value (yellow-blue coordinate) as a function of aging time for samples with plasticizer contents of 10 wt% (b), 20 wt% (c), and 30 wt% (d); (e) Comparison of Δb^* values after aging for 190 min.

influence of specific molecular structures and substitution modes.[42]

EACHDMR, bearing two hydroxymethyl groups (—CH_2OH) on the cyclohexane ring, exhibited the most balanced and superior performance. Its symmetric structure and extended, flexible —CH_2— spacers between the rigid core and ester linkages are important.[49,50] This configuration may enable the molecule to form an optimal conformation that considers both steric hindrance and compatibility. Its large-volume core can effectively separate the PVC chains to inhibit migration. The —CH_2— spacer and epoxy groups provide the necessary flexibility and polarity, enabling uniform interaction with the polymer matrix and promoting chain mobility, thereby achieving the highest plasticizing efficiency and durability.

https://doi.org/10.1007/s10118-026-3698-2

In contrast, EACHR demonstrates outstanding plasticizing ability owing to the direct connection of a single hydroxyl group (—OH) on its ring, but its anti-migration property is slightly reduced compared to EACHDMR. This asymmetric structure can enhance its ability to be inserted into the PVC chains, thereby explaining its high efficiency. However, their smaller rigid dimensions and lower symmetry may offer poorer resistance to migration, which represents a delicate trade-off in the design structure.

The performance of the EACHDR highlights a critical design limit. Although it contains a cyclohexane ring, its two hydroxyl groups (—OH) are attached directly to the ring in a vicinal (1,4-) configuration. This may result in the formation of a highly polar and conformally restricted region. We posit that this strong polarity might lead to poor dispersion in regions with lower polarity within the PVC matrix, thereby reducing overall compatibility.[51] In addition, the lack of flexible $-CH_2-$ spacers may limit the ability of the molecule to effectively screen PVC dipole-dipole interactions in a larger volume, restrict its plasticizing effect, and make it more prone to migration.

From this analysis, possible guiding principles for the molecular design of sustainable plasticizers emerge: (1) a bio-derived, alicyclic rigid core as an effective and non-toxic substitute for benzene rings mainly enhances stability by endowing steric hindrance. (2) The specific functionalization of this core is a key determinant of the overall performance. A balance among optimizing the steric bulk, molecular flexibility, and polarity is indispensable. This not only requires a core structure but also regulates its interaction with the polymer matrix by choosing the appropriate substituents.

CONCLUSIONS

This study validates a novel molecular design strategy for balancing performance and sustainability. Based on the synergistic integration of a bio-derived cyclohexane rigid core, flexible non-edible ricinoleic acid (RA) backbone, and epoxy groups, this strategy was effectively implemented in the synthesis of plasticizers. The best plasticizer, EACHDMR, is a prime example of this design with an overall performance comparable to or even surpassing that of the commercial benchmark dioctyl terephthalate (DOTP). Notably, it exhibits excellent plasticizing efficiency, good resistance to migration and volatilization, and good thermal stability. Its incorporation into PVC delivered enhanced mechanical properties, increasing the elongation at break by more than 50-fold and the notched impact strength by more than 35-fold, while lowering the glass transition temperature by 30%. Mechanistically, this performance stems from the synergy between the three design elements. The steric hindrance provided by the rigid cyclohexane skeleton inhibited migration. The polar interaction of epoxy groups and the flexible synergistic effect provided by the long-chain structure jointly enhance compatibility and chain mobility. Therefore, this work not only provides alternative solutions for petroleum-based plasticizers, but also offers some references for the molecular design of sustainable plasticizers.

Conflict of Interests

The authors declare no interest conflict.

Data Availability Statement

The data supporting the findings of this study are available from the corresponding author upon reasonable request.

ACKNOWLEDGMENTS

This work was financially supported by the Jilin Provincial Scientific and Technological Development Program (No. 20240301030GX) and the Changchun Science and Technology Planning Project (No. 24GXYSZZ41).

REFERENCES

1 Wang, Y.; Qian, H. Phthalates and their impacts on human health. *Healthcare.* **2021**, *9*, 603.
2 Zia, A. I.; Abdul Rahman, M. S.; Mukhopadhyay, S. C.; Yu, P. L.; Al-Bahadly, I.; Gooneratne, C.; Kosel, J.; Taishan, L. Electrochemical impedance spectroscopy based MEMS sensors for phthalates detection in water and juices. *J. Phys. Conf. Ser.* **2013**, *439*, 012026.
3 Sabi, G. J.; Simões, A .L. A.; Gorup, L. F.; da Silva, W. A.; Mendes, A. A. Production of benzyl-based esters from used soybean cooking oil as renewable plasticizers for flexible PVC films: Exploring new applications for lipases in emerging technologies. *Int. J. Biol. Macromol.* **2025**, *292*, 139233.
4 Yang, Y.; Tao, Y.; Yang, R.; Yi, X.; Zhong, G.; Gu, Y.; Zhang, Y. Ca2+ homeostasis imbalance induced by Pparg: A key factor in di (2-ethylhexyl) phthalate (DEHP)-induced cardiac dysfunction in zebrafish larvae. *Sci. Total Environ.* **2024**, *918*, 170436.
5 Mo, L.; Fang, L.; Yao, W.; Nie, J.; Dai, J.; Liang, Y.; Qin, L. LC-QTOF/MS-based non-targeted metabolomics to explore the toxic effects of di(2-ethylhexyl) phthalate (DEHP) on Brassica chinensis L. *Sci Total Environ.* **2024**, *918*, 170817.
6 Gao, X.; Cui, L.; Mu, Y.; Li, J.; Zhang, Z.; Zhang, H.; Xing, F.; Duan, L.; Yang, J. Cumulative health risk in children and adolescents exposed to bis(2-ethylhexyl) phthalate (DEHP). *Environ Res.* **2023**, *237*, 116865.
7 Fiorentino, G.; Ripa, M.; Ulgiati, S. Chemicals from biomass: technological versus environmental feasibility. A review. *Biofuels.* **2017**, *11*, 195–214.
8 Djouonkep, L.D.W.; Tamo, C.T.; Simo, B.E.; Issah, N.; Tchouagtie, M.N.; Selabi, N.B.S.; Doench, I.; Kamdem Tamo, A.; Xie, B.; Osorio-Madrazo, A. Synthesis by melt-polymerization of a novel series of bio-based and biodegradable thiophene-containing copolyesters with promising gas barrier and high Thermomechanical Properties. *Molecules.* **2023**, *28*, 1825.
9 Mujtaba, M.; Lipponen, J.; Ojanen, M.; Puttonen, S.; Vaittinen, H. Trends and challenges in the development of bio-based barrier coating materials for paper/cardboard food packaging; a review. *Sci Total Environ.* **2022**, *851*, 158328.
10 Li, D.; Panchal, K.; Vasudevan, N.; Mafi, R.; Xi, L. Effects of molecular design parameters on plasticizer performance in poly(vinyl chloride): a comprehensive molecular simulation study. **2021**, *249*, 117334.
11 Chen, Y.; Zhou, S.; Pan, S.; Zhao, D.; Wei, J.; Zhao, M.; Fan, H. Methods for determination of plasticizer migration from

Graphical Abstract

Epoxy-functionalized Cyclohexane-based Ricinoleate Plasticizer: Synthesis, Performance Evaluation, and Plasticizing Mechanism

Zhuo-Kai Wang, Ying-Yong Jiang, Wen-Nan Du, Yao-Bin Wang, Xing-Chen Bai, Cheng-Wei Song, Zhi-Peng Jiang, Liang Ren, Sai-Nan Cui, and Feng-Xiang Gao

Changchun University of Technology; Research Institute of Jilin Petrochemical Company, PetroChina; Institute of Applied Chemistry CAS, Chinese Academy of Sciences

A novel molecular design integrating flexible non-edible backbone, alicyclic rigid core, and epoxy groups breaks the performance-sustainability trade-off. The optimal plasticizer lowers poly(vinyl chloride) (PVC) T_g by 30%, increases elongation >50-fold, and improves efficiency by 20.7% versus DOTP.

Chinese J. Polym. Sci., 2026 *https://doi.org/10.1007/s10118-026-3698-2*

polyvinyl chloride synthetic materials: a mini review. *J. Leather Sci. Eng.* **2022**, *4*, 8.

12 Rahman, M.; Brazel, C.S. The plasticizer market: an assessment of traditional plasticizers and research trends to meet new challenges. *Prog. Polym. Sci.* **2004**, *29*, 1223–1248.

13 He, W.; Zhu, G.; Gao, Y.; Wu, H.; Fang, Z.; Guo, K. Green plasticizers derived from epoxidized soybean oil for poly (vinyl chloride): Continuous synthesis and evaluation in PVC films. *Chem. Eng. J.* **2020**, *380*, 122532.

14 Quiles-Carrillo, L.; Duart, S.; Montanes, N.; Torres-Giner, S.; Balart, R. Enhancement of the mechanical and thermal properties of injection-molded polylactide parts by the addition of acrylated epoxidized soybean oil. *Mater. Des.* **2018**, *140*, 54–63.

15 Feng, G. D.; Hu, Y.; Zhou, Y. H. Preparation and application of epoxy oil-based fire-retardant plasticizer for PVC. *Asian J. Chem.* **2015**, *19*, S5–481-S5-485.

16 Ma, Y.; Kou, Z.; Jia, P.; Zhou, J. Effect of benzene ring and alkane chain contained bio-based plasticizers on the plasticizing performance of polyvinyl chloride films. *Chem. Pap.* **2021**, *75*, 5515–5521.

17 Hou, B.; Wang, Y.; Li, B.; Gong, T.; Wu, J.; Li, J. Synthesis of novel L-lactic acid-based plasticizers and their effects on the flexibility, crystallinity, and optical transparency of poly(lactic acid). *Int. J. Biol. Macromol.* **2024**, *273*, 132826.

18 Tan, S.X.; Andriyana, A.; Ong, H.C.; Lim, S.; Pang, Y.L.; Ngoh, G.C. A comprehensive review on the emerging roles of nanofillers and plasticizers towards sustainable starch-based bioplastic fabrication. *Polymers.* **2022**, *14*, 664.

19 Amri, M.; Al-Edrus, S.; Luqman Chuah, A.; Md Yasin, F.; Lee, S.H. Jatropha oil as a substituent for palm oil in biobased polyurethane. *Int. J. Polym. Sci.* **2021**, *2021*, 6655936.

20 Caicho-Caranqui, J.; Taipe, L.A.; Mena, K.A.; Ponce, S.; Mora, J.R.; Negrete-Bolagay, D.; Zamora-Mendoza, L.; Guerrero, V.H.; Ponton Bravo, P.I.; Pasquel, D.; Paredes, J.; Alvarez Barreto, J.F.; Zambrano, C.; Alexis, F. Towards sustainable bioplasticizers from biomass to polymers applications: a review. *Sustain. Mater. Technol.* **2025**, *43*, e01194.

21 Zhang, Z.; Jiang, P.; Liu, D.; Feng, S.; Zhang, P.; Wang, Y.; Fu, J.; Agus, H. Research progress of novel bio-based plasticizers and their applications in poly(vinyl chloride). *J. Mater. Sci.* **2021**, *56*, 10155–10182.

22 Deshmukh, A.; Ganure, V. A review of the literature on eranda(Ricinus Communis Linn.,) and its therapeutic applications and phytochemical components. *Int. Ayurved. Med. J.* **2023**, *11*,

1249–1254.
23 Dwivedi, N.N.; Sharma, R. A Beneficial Action of Ricinus Communis. *Int. J. Res. Rev.* **2022**, *9*, 159–168.
24 Jia, P.; Hu, L.; Zhang, M.; Feng, G.; Zhou, Y. Phosphorus containing castor oil based derivatives: potential non-migratory flame retardant plasticizer. *Eur. Polym. J.* **2017**, *87*, 209–220.
25 Yamamoto, A.; Nemoto, K.; Yoshida, M.; Tominaga, Y.; Imai, Y.; Ata, S.; Takenaka, Y.; Abe, H.; Sato, K. Improving thermal and mechanical properties of biomass-based polymers using structurally ordered polyesters from ricinoleic acid and 4-hydroxycinnamic acids. *RSC Adv.* **2020**, *10*, 36562–36570.
26 Jing, Y.; Xia, Q.; Xie, J.; Liu, X.; Guo, Y.; Zou, J. J.; Wang, Y. Robinson annulation-directed synthesis of jet-fuel-ranged alkylcyclohexanes from biomass-derived chemicals. *ACS Catal.* **2018**, *8*, 3280–3285.
27 Li, X.; Guo, T.; Xia, Q.; Liu, X.; Wang, Y. One-pot catalytic transformation of lignocellulosic biomass into alkylcyclohexanes and polyols. *ACS Sustain. Chem. Eng.* **2018**, *6*, 4390–4399.
28 Chaiyaraksa, C.; Sriprom, P.; Boonkaen, F.; Laemsri, A.; Smingkaew, A.; Chokelarb, W.; Assawasaengrat, P. Cleaner bio-based plasticizer synthesis from waste cooking oil to substitute toxic dioctyl phthalate in PVC film. *Key Eng. Mater.* **2025**, *1017*, 103–108.
29 Cruz, P.P.R.; da Silva, L.C.; Fiuza-Jr, R.A.; Polli, H. Thermal dehydrochlorination of pure PVC polymer: Part I—thermal degradation kinetics by thermogravimetric analysis. *J. Appl. Polym. Sci.* **2021**, *138*, e50598.
30 Yu, J.; Sun, L.; Ma, C.; Qiao, Y.; Yao, H. Thermal degradation of PVC: a review. *Waste Manag.* **2016**, *48*, 300–314.
31 Kwon, C.W.; Chang, P.-S. Influence of alkyl chain length on the action of acetylated monoglycerides as plasticizers for poly (vinyl chloride) food packaging film. *Food Packag. Shelf Life.* **2021**, *27*, 100619.
32 Qian, B.; Zhang, J.; Wu, M.; Liu, J.; Wu, Q.; Yang, J. Synthesis, characterization and performance evaluation of "crab" bio-based poly(vinyl chloride) plasticizer based on sustainable lactic acid. *Polymer.* **2023**, *283*, 126246.
33 Jia, P.; Hu, L.; Shang, Q.; Wang, R.; Zhang, M.; Zhou, Y. Self-Plasticization of PVC materials via chemical modification of mannich base of cardanol butyl ether. *ACS Sustain. Chem. Eng.* **2017**, *5*, 6665–6673.
34 Cai, D. L.; Yue, X.; Hao, B.; Ma, P. C. A sustainable poly(vinyl chloride) plasticizer derivated from waste cooking oil. *J. Clean. Prod.* **2020**, *274*, 122781.
35 Guan, C.; Xiao, C.; Liu, X.; Hu, Z.; Wang, R.; Wang, C.; Xie, C.; Cai, Z.; Li, W. Non-Covalent interactions between polyvinyl chloride and conjugated polymers enable excellent mechanical properties and high stability in organic solar cells. *Angew. Chem. Int. Ed.* **2023**, *62*, e202312357.
36 Fox, T.G., Jr.; Flory, P.J. Second-order transition temperatures and related properties of polystyrene. I. Influence of Molecular Weight. *J. Appl. Phys.* **1950**, *21*, 581–591.
37 Xuan, W.; Hakkarainen, M.; Odelius, K. Levulinic acid as a versatile building block for plasticizer design. *ACS Sustain. Chem. Eng.* **2019**, *7*, 12552–12562.
38 Lenzi, L.; Degli Esposti, M.; Braccini, S.; Siracusa, C.; Quartinello, F.; Guebitz, G.M.; Puppi, D.; Morselli, D.; Fabbri, P. Further step in the transition from conventional plasticizers to versatile bioplasticizers obtained by the valorization of levulinic acid and glycerol. *ACS Sustain. Chem. Eng.* **2023**, *11*, 9455–9469.
39 Edo, G. I.; Ndudi, W.; Ali, A. B. M.; Yousif, E.; Zainulabdeen, K.; Onyibe, P. N.; Ekokotu, H. A.; Isoje, E. F.; Igbuku, U. A.; Essaghah, A. E. A.; Ahmed, D. S.; Umar, H.; Ozsahin, D.U. Poly(vinyl chloride) (PVC): an updated review of its properties, polymerization, modification, recycling, and applications. *J. Mater. Sci.* **2024**, *59*, 21605–21648.
40 Daniels, P. A brief overview of theories of PVC plasticization and methods used to evaluate PVC-Plasticizer interaction. *J. Vinyl Addit. Technol.* **2009**, *15*, 219–223.
41 Zhou, H.; Xu, P.; Xie, S.; Feng, Z.; Wang, D. Mechanical performance and energy absorption properties of structures combining two Nomex honeycombs. *Compos. Struct.* **2018**, *185*, 524–536.
42 Jiang, Y.; Gao, F.; Ren, L.; Liu, Q.; Song, T.; Shen, Y.; Du, W.; Wang, Y.; Zhang, M. Novel environmentally sustainable plasticizers based on ricinoleic acid for poly(vinyl chloride): structure and properties. *New J. Chem.* **2024**, *48*, 4960–4975.
43 Lourdin, D.; Coignard, L.; Bizot, H.; Colonna, P. Influence of equilibrium relative humidity and plasticizer concentration on the water content and glass transition of starch materials. *Polymer.* **1997**, *38*, 5401–5406.
44 Burns, K.; Potgieter, J.H.; Potgieter-Vermaak, S.; Ingram, I.; Liauw, C. A comparative assessment of the use of suitable analytical techniques to evaluate plasticizer compatibility. *J. Appl. Polym. Sci.* **2023**, *140*, 54104.
45 O'Mahony, C. T.; Borah, D.; Morris, M. A. Microphase separation of a PS-b-PFS block copolymer via solvent annealing: effect of solvent, substrate, and exposure time on morphology. *Int. J. Polym. Sci.* **2015**, *2015*, 270891.
46 Mackey, J.; Grover, D.; Pruneda, G.; Zenk, E.; Nagy, Z. K. Continuous extraction of 2-chloroethyl isocyanate for 1-(2-chloroethyl)-3-cyclohexylurea purification. *Chem. Eng. Process. Process Intensif.* **2023**, *183*, 109225.
47 Yang, Y.; Zhang, C. L.; Han, Y.; Weng, Y. X. Plasticizing and thermal stabilizing effect of bio-based epoxidized cardanol esters on PVC. *Polym. Adv. Technol.* **2022**, *34*, 181–194.
48 Sun, S. Y.; Weng, Y. X.; Zhang, C. L. Recent advancements in bio-based plasticizers for polylactic acid (PLA): a review. *Polym. Test.* **2024**, *140*, 108603.
49 Abou-Rachid, H.; Lussier, L.-S.; Ringuette, S.; Lafleur-Lambert, X.; Jaidann, M.; Brisson, J. On the correlation between miscibility and solubility properties of energetic plasticizers/polymer blends: modeling and simulation studies. *Propellants Explos. Pyrotech.* **2008**, *33*, 301–310.
50 Yang, W.; Chen, X.; Song, X.; Hu, Y.; Pei, J.; Chen, J. Molecular dynamics study on the physical compatibility of SEBS/plasticizer blend systems. *J. Mol. Model.* **2024**, *30*, 293.
51 Jarray, A.; Gerbaud, V.; Hemati, M. Polymer-plasticizer compatibility during coating formulation: A multi-scale investigation. *Prog. Org. Coat.* **2016**, *101*, 195–206.